

Measurements of the D_{sJ} resonance properties

Y. Mikami,³⁸ K. Abe,⁷ T. Abe,⁷ H. Aihara,³⁹ M. Akemoto,⁷ Y. Asano,⁴⁴ T. Aso,⁴³ T. Aushev,¹¹ S. Bahinipati,⁴ A. M. Bakich,³⁴ Y. Ban,²⁹ A. Bay,¹⁶ I. Bizjak,¹² A. Bondar,² A. Bozek,²³ M. Bračko,^{18,12} T. E. Browder,⁶ Y. Chao,²² B. G. Cheon,³³ R. Chistov,¹¹ S.-K. Choi,⁵ Y. Choi,³³ Y. K. Choi,³³ A. Chuvikov,³⁰ M. Danilov,¹¹ L. Y. Dong,⁹ J. Dragic,¹⁹ S. Eidelman,² V. Eiges,¹¹ C. Fukunaga,⁴¹ K. Furukawa,⁷ N. Gabyshev,⁷ A. Garmash,^{2,7} T. Gershon,⁷ G. Gokhroo,³⁵ B. Golob,^{17,12} F. Handa,³⁸ T. Hara,²⁷ H. Hayashii,²¹ M. Hazumi,⁷ I. Higuchi,³⁸ L. Hinz,¹⁶ T. Hokuue,²⁰ Y. Hoshi,³⁷ W.-S. Hou,²² H.-C. Huang,²² T. Iijima,²⁰ H. Ikeda,⁷ K. Inami,²⁰ A. Ishikawa,²⁰ H. Iwasaki,⁷ M. Iwasaki,³⁹ Y. Iwasaki,⁷ J. H. Kang,⁴⁷ J. S. Kang,¹⁴ P. Kapusta,²³ N. Katayama,⁷ H. Kawai,³ N. Kawamura,¹ T. Kawasaki,²⁵ H. Kichimi,⁷ E. Kikutani,⁷ H. J. Kim,⁴⁷ J. H. Kim,³³ K. Kinoshita,⁴ P. Koppenburg,⁷ P. Krizan,^{17,12} P. Krokovny,² R. Kulasiri,⁴ Y.-J. Kwon,⁴⁷ G. Leder,¹⁰ S. H. Lee,³² T. Lesiak,²³ S.-W. Lin,²² D. Liventsev,¹¹ J. MacNaughton,¹⁰ F. Mandl,¹⁰ M. Masuzawa,⁷ T. Matsumoto,⁴¹ A. Matyja,²³ T. Mimashi,⁷ W. Mitaroff,¹⁰ H. Miyata,²⁵ G. R. Moloney,¹⁹ T. Nagamine,³⁸ Y. Nagasaka,⁸ T. T. Nakamura,⁷ E. Nakano,²⁶ M. Nakao,⁷ H. Nakazawa,⁷ Z. Natkaniec,²³ S. Nishida,⁷ O. Nitoh,⁴² T. Nozaki,⁷ S. Ogawa,³⁶ Y. Ogawa,⁷ K. Ohmi,⁷ T. Ohshima,²⁰ N. Ohuchi,⁷ K. Oide,⁷ T. Okabe,²⁰ S. Okuno,¹³ S. L. Olsen,⁶ W. Ostrowicz,²³ H. Ozaki,⁷ P. Pakhlov,¹¹ H. Palka,²³ C. W. Park,¹⁴ H. Park,¹⁵ K. S. Park,³³ N. Parslow,³⁴ L. E. Piilonen,⁴⁵ H. Sagawa,⁷ S. Saitoh,⁷ Y. Sakai,⁷ O. Schneider,¹⁶ C. Schwanda,^{7,10} A. J. Schwartz,⁴ S. Semenov,¹¹ K. Senyo,²⁰ M. E. Sevier,¹⁹ H. Shibuya,³⁶ T. Shidara,⁷ B. Shwartz,² V. Sidorov,² J. B. Singh,²⁸ N. Soni,²⁸ S. Stanič,^{44,*} M. Starič,¹² R. Sugahara,⁷ A. Sugi,²⁰ K. Sumisawa,²⁷ T. Sumiyoshi,⁴¹ S. Suzuki,⁴⁶ S. Y. Suzuki,⁷ F. Takasaki,⁷ M. Tanaka,⁷ M. Tawada,⁷ Y. Teramoto,²⁶ T. Tomura,³⁹ K. Trabelsi,⁶ T. Tsuboyama,⁷ T. Tsukamoto,⁷ S. Uehara,⁷ S. Uno,⁷ G. Varner,⁶ Y. Watanabe,⁴⁰ B. D. Yabsley,⁴⁵ Y. Yamada,⁷ A. Yamaguchi,³⁸ H. Yamamoto,³⁸ Y. Yamashita,²⁴ M. Yamauchi,⁷ H. Yanai,²⁵ Heyoung Yang,³² J. Ying,²⁹ M. Yoshida,⁷ Y. Yusa,³⁸ Z. P. Zhang,³¹ V. Zhilich,² and D. Žontar^{17,12}

(The Belle Collaboration)

¹*Aomori University, Aomori*

²*Budker Institute of Nuclear Physics, Novosibirsk*

³*Chiba University, Chiba*

⁴*University of Cincinnati, Cincinnati, Ohio 45221*

⁵*Gyeongsang National University, Chinju*

⁶*University of Hawaii, Honolulu, Hawaii 96822*

⁷*High Energy Accelerator Research Organization (KEK), Tsukuba*

⁸*Hiroshima Institute of Technology, Hiroshima*

⁹*Institute of High Energy Physics, Chinese Academy of Sciences, Beijing*

¹⁰*Institute of High Energy Physics, Vienna*

¹¹*Institute for Theoretical and Experimental Physics, Moscow*

¹²*J. Stefan Institute, Ljubljana*

¹³*Kanagawa University, Yokohama*

¹⁴*Korea University, Seoul*

¹⁵*Kyungpook National University, Taegu*

¹⁶*Institut de Physique des Hautes Énergies, Université de Lausanne, Lausanne*

¹⁷*University of Ljubljana, Ljubljana*

¹⁸*University of Maribor, Maribor*

¹⁹*University of Melbourne, Victoria*

²⁰*Nagoya University, Nagoya*

²¹*Nara Women's University, Nara*

²²*Department of Physics, National Taiwan University, Taipei*

²³*H. Niewodniczanski Institute of Nuclear Physics, Krakow*

²⁴*Nihon Dental College, Niigata*

²⁵*Niigata University, Niigata*

²⁶*Osaka City University, Osaka*

²⁷*Osaka University, Osaka*

²⁸*Panjab University, Chandigarh*

²⁹*Peking University, Beijing*

³⁰*Princeton University, Princeton, New Jersey 08545*

³¹*University of Science and Technology of China, Hefei*

³²Seoul National University, Seoul

³³Sungkyunkwan University, Suwon

³⁴University of Sydney, Sydney NSW

³⁵Tata Institute of Fundamental Research, Bombay

³⁶Toho University, Funabashi

³⁷Tohoku Gakuin University, Tagajo

³⁸Tohoku University, Sendai

³⁹Department of Physics, University of Tokyo, Tokyo

⁴⁰Tokyo Institute of Technology, Tokyo

⁴¹Tokyo Metropolitan University, Tokyo

⁴²Tokyo University of Agriculture and Technology, Tokyo

⁴³Toyama National College of Maritime Technology, Toyama

⁴⁴University of Tsukuba, Tsukuba

⁴⁵Virginia Polytechnic Institute and State University, Blacksburg, Virginia 24061

⁴⁶Yokkaichi University, Yokkaichi

⁴⁷Yonsei University, Seoul

We report measurements of the properties of the $D_{sJ}^+(2317)$ and $D_{sJ}^+(2457)$ resonances produced in continuum e^+e^- annihilation near $\sqrt{s} = 10.6$ GeV. The analysis is based on an 86.9 fb^{-1} data sample collected with the Belle detector at KEKB. We determine the masses to be $M(D_{sJ}^+(2317)) = 2317.2 \pm 0.5(\text{stat}) \pm 0.9(\text{syst}) \text{ MeV}/c^2$ and $M(D_{sJ}^+(2457)) = 2456.5 \pm 1.3(\text{stat}) \pm 1.3(\text{syst}) \text{ MeV}/c^2$. We observe the radiative decay mode $D_{sJ}^+(2457) \rightarrow D_s^+ \gamma$ and the dipion decay mode $D_{sJ}^+(2457) \rightarrow D_s^+ \pi^+ \pi^-$, and determine their branching fractions. No corresponding decays are observed for the $D_{sJ}(2317)$ state. These results are consistent with the spin-parity assignments of 0^+ for the $D_{sJ}(2317)$ and 1^+ for the $D_{sJ}(2457)$.

PACS numbers: 13.25.Hw, 14.40.Nd

The narrow $D_s \pi^0$ resonance at $2317 \text{ MeV}/c^2$, recently observed by the BaBar collaboration [1], is naturally interpreted as a P-wave excitation of the $c\bar{s}$ system. The observation of a nearby and narrow $D_s^* \pi^0$ resonance by the CLEO collaboration [2] supports this view, since the mass difference of the two observed states is consistent with the expected hyperfine splitting for a P-wave doublet with total light-quark angular momentum $j = 1/2$ [3, 4]. The observed masses are, however, considerably lower than potential model predictions [6] and similar to those of the $c\bar{u}$ $j = 1/2$ doublet states recently reported by Belle [7]. This has led to speculation that the new $D_s^{(*)} \pi^0$ resonances, which we denote D_{sJ} , may be exotic mesons [8, 9, 10, 11, 12, 13]. Measurements of the D_{sJ} quantum numbers and branching fractions (particularly those for radiative decays), will play an important role in determining the nature of these states.

In this paper we report measurements of the D_{sJ} masses, widths and branching fractions using a sample of $e^+e^- \rightarrow c\bar{c}$ events collected with the Belle detector [14] at the KEKB collider [15].

We reconstruct D_s^+ mesons using the decay chain $D_s^+ \rightarrow \phi \pi^+$ and $\phi \rightarrow K^+ K^-$. To identify kaons or pions, we form a likelihood for each track, $\mathcal{L}_{K(\pi)}$, from dE/dx measurements in a 50-layer central drift chamber, the responses from aerogel threshold Čerenkov counters, and time-of-flight scintillation counters. The kaon likelihood ratio, $P(K/\pi) = \mathcal{L}_K / (\mathcal{L}_K + \mathcal{L}_\pi)$, has values between 0 (likely to be a pion) and 1 (likely to be a kaon).

For $\phi \rightarrow K^+ K^-$ candidates we use oppositely-charged track pairs where one track has $P(K/\pi) > 0.5$ and the

other has $P(K/\pi) > 0.2$, and with a $K^+ K^-$ invariant mass that is within $10 \text{ MeV}/c^2$ ($\sim 2.5\sigma$) of the nominal ϕ mass. We define the ϕ helicity angle θ_H to be the angle between the direction of the K^+ and the D_s^+ in the ϕ rest frame. For signal events this has a $\cos^2 \theta_H$ distribution, while for background it is flat; we require $|\cos \theta_H| > 0.35$.

We reconstruct D_s^+ candidates by combining a ϕ candidate with a π^+ , which is a charged track with $P(K/\pi) < 0.9$, and requiring $M(\phi \pi^+)$ to be within $10 \text{ MeV}/c^2$ ($\sim 2\sigma$) of the nominal D_s^+ mass. We use the D_s^+ sideband regions $1920 < M(\phi \pi^+) < 1940 \text{ MeV}/c^2$ and $1998 < M(\phi \pi^+) < 2018 \text{ MeV}/c^2$ for background studies.

For π^0 reconstruction, we use photons with the e^+e^- rest frame (CM) energies greater than 100 MeV and select $\gamma\gamma$ pairs that have an invariant mass $M(\gamma\gamma)$ within $10 \text{ MeV}/c^2$ ($\sim 2\sigma$) of the π^0 mass. For background studies we use the π^0 sideband regions $105 \leq M_{\gamma\gamma} \leq 115 \text{ MeV}/c^2$ and $155 \leq M_{\gamma\gamma} \leq 165 \text{ MeV}/c^2$.

We reconstruct D_s^{*+} in the $D_s^+ \gamma$ final state. We use photons with CM energies greater than 100 MeV and require D_s^{*+} candidates to satisfy $127 \leq \Delta M(D_s^+ \gamma) \leq 157 \text{ MeV}/c^2$ ($\sim 3\sigma$), where $\Delta M(D_s^+ \gamma) = M(D_s^+ \gamma) - M_{D_s^+}$. The D_s^{*+} sideband regions are defined as $87 \leq \Delta M(D_s^+ \gamma) \leq 117 \text{ MeV}/c^2$ and $167 \leq \Delta M(D_s^+ \gamma) \leq 197 \text{ MeV}/c^2$.

The $\Delta M(D_s^+ \pi^0) = M(D_s^+ \pi^0) - M_{D_s^+}$ mass-difference distribution for $D_s^+ \pi^0$ combinations with $p^*(D_s^+ \pi^0) > 3.5 \text{ GeV}/c$ is shown in Fig. 1(a). Here, and in analyses of other D_{sJ} states and modes, we require the CM momentum to satisfy $p^*(D_{sJ}) > 3.5 \text{ GeV}/c$ to remove

contributions from $B\bar{B}$ events. We do not remove multiple candidates in the subsequent analysis. Also shown are the distributions for the D_s^+ (solid) and π^0 (dashed) sideband regions. The prominent peak in the figure corresponds to the $D_{sJ}(2317) \rightarrow D_s^+\pi^0$ signal; the peak at small ΔM values is due to $D_s^{*+}(2112) \rightarrow D_s^+\pi^0$. No peak is seen in the sideband distributions.

Figure 1(b) shows the $\Delta M(D_s^{*+}\pi^0) = M(D_s^{*+}\pi^0) - M_{D_s^{*+}}$ distribution for $p^*(D_s^{*+}\pi^0) > 3.5 \text{ GeV}/c$, where a peak corresponding to $D_{sJ}(2457) \rightarrow D_s^{*+}\pi^0$ is evident. Also shown is the distribution for the D_s^{*+} sideband region, where we notice the presence of a wider peak in the $D_{sJ}(2457)$ region. The $\Delta M(D_s^{*+}\pi^0)$ distributions for the D_s^+ and π^0 sideband regions show no such peak.

To study the expected signal shape and detection efficiencies, and determine the level of cross-feed between the two states, we use a Monte Carlo simulation that treats the $D_{sJ}(2317)$ as a scalar particle with mass $2317 \text{ MeV}/c^2$ decaying to $D_s^+\pi^0$ and the $D_{sJ}(2457)$ as an axial-vector particle with mass $2457 \text{ MeV}/c^2$ decaying to $D_s^{*+}\pi^0$. Zero intrinsic width is assigned to both states. We find that the $D_{sJ}(2317)$ produces a peak of width $7.1 \pm 0.2 \text{ MeV}/c^2$ in the $\Delta M(D_s^+\pi^0)$ distribution at its nominal mass, and a broader reflection peak (of width $12.3 \pm 1.8 \text{ MeV}/c^2$) at a mass of $8 \text{ MeV}/c^2$ above the $D_{sJ}(2457)$ peak. This latter peak corresponds to a D_s^+ and π^0 from a $D_{sJ}(2317)$ decay that are combined with a random photon that passes the $|M(D_s^+\gamma) - M_{D_s^{*+}}| < 15 \text{ MeV}/c^2$ requirement. (We refer to this as “feed-up background.”) The $D_{sJ}(2457)$ produces a peak of width $6.0 \pm 0.2 \text{ MeV}/c^2$ at its nominal mass and a broader peak (of width $19.5 \pm 3.6 \text{ MeV}/c^2$), also at its nominal mass. The latter peak is due to events in which the photon from $D_s^{*+} \rightarrow D_s^+\gamma$ is missed, and a random photon is reconstructed in its place (referred to as the “broken-signal background”). In addition, the $D_{sJ}(2457)$ produces a reflection in the $D_s^+\pi^0$ mass distribution with width $14.9 \pm 0.8 \text{ MeV}/c^2$ at a mass of $4 \text{ MeV}/c^2$ below the $D_{sJ}(2317)$ peak (referred to as “feed-down background”).

While we must depend on the MC for separating the signal peak and the feed-down background in the $D_{sJ}(2317)$ region, the feed-up and broken-signal backgrounds for the $D_{sJ}(2457)$ region occur when $D_s^{*+}\pi^0$ combinations are formed from candidates in the D_s^{*+} mass sideband. This is evident in Fig. 1(b).

Figure 2(b) shows the sideband-subtracted $\Delta M(D_s^{*+}\pi^0)$ distribution together with the results of a fit that uses a Gaussian to represent the $D_{sJ}(2457)$ signal and a second-order polynomial for the background. The fit gives a signal yield of 126 ± 25 events with a peak value of $\Delta M = 344.1 \pm 1.3 \text{ MeV}/c^2$ (corresponding to $M = 2456.5 \pm 1.3 \text{ MeV}/c^2$). The width from the fit, $\sigma = 5.8 \pm 1.3 \text{ MeV}/c^2$, is consistent with MC expectations for a zero intrinsic width particle.

Figure 2(a) shows the fit result for the $D_{sJ}(2317)$.

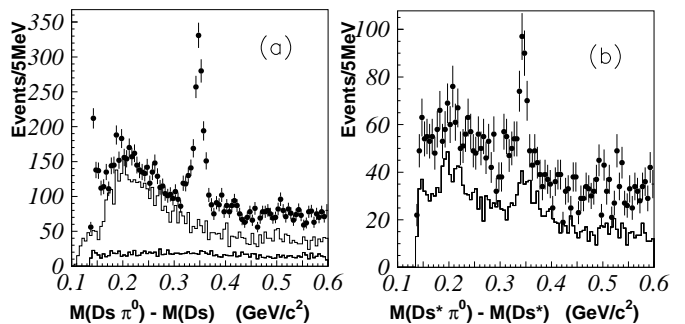


FIG. 1: (a) The $\Delta M(D_s^+\pi^0)$ distribution. Data from the D_s^+ (solid) and π^0 (dashed) sideband regions are also shown. (b) The $\Delta M(D_s^{*+}\pi^0)$ distribution. Data from the D_s^* sideband (histogram) region is also shown.

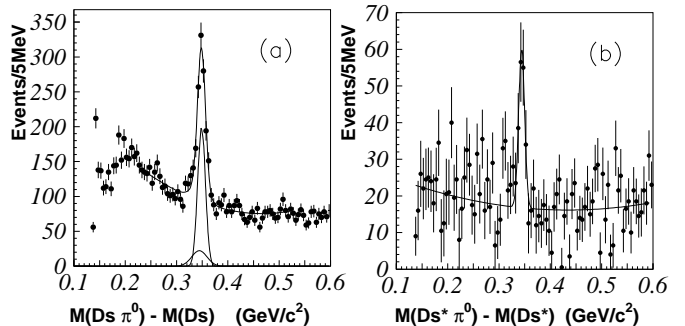


FIG. 2: (a) The $\Delta M(D_s^+\pi^0)$ distribution. The narrow Gaussian peak is the fitted $D_{sJ}(2317)$ signal, whereas the wider Gaussian peak is the feed-down background. (b) The $\Delta M(D_s^{*+}\pi^0)$ distribution after bin-by-bin subtraction of the D_s^{*+} sideband from the D_s^{*+} signal distribution. The curve is the fit result.

Here both the signal and the feed-down background are represented as Gaussian shapes modeled from the MC. The mean and σ of the feed-down component are fixed according to the MC and normalized by the measured $D_{sJ}(2457)$ yield. A third-order polynomial is used to represent the non-feed-down background. The fit gives a yield of 761 ± 44 events and a peak ΔM value of $348.7 \pm 0.5 \text{ MeV}/c^2$ (corresponding to $M = 2317.2 \pm 0.5 \text{ MeV}/c^2$). Here again, the width from the fit, $\sigma = 7.6 \pm 0.5 \text{ MeV}/c^2$, is consistent with MC expectations for a zero intrinsic width particle.

There are systematic errors in the measurements due to uncertainties in the: i) π^0 energy calibration; ii) parameterization of the cross-feed backgrounds; iii) parameterization for the non-cross-feed backgrounds; iv) possible discrepancies between the input and output seen in the MC simulations; and v) the uncertainty in the world average value for $M_{D_s^+}$ and $M_{D_s^{*+}}$.

The π^0 energy calibration is studied using $D_s^{*+}(2112) \rightarrow D_s^+\pi^0$ events in the same data sample. We measure $\Delta M = 144.3 \pm 0.1 \text{ MeV}/c^2$ and $\sigma = 1.0 \pm 0.1 \text{ MeV}/c^2$, which agrees well with the

PDG value of $\Delta M = 143.8 \pm 0.4 \text{ MeV}/c^2$. The MC, which uses the PDG value as an input, gives $\Delta M = 143.9 \pm 0.1 \text{ MeV}/c^2$ and $\sigma = 1.0 \pm 0.1 \text{ MeV}/c^2$. (The errors quoted here are statistical only). We attribute the difference to the π^0 energy calibration uncertainty, and conservatively assign a $\pm 0.6 \text{ MeV}/c^2$ error to this effect. This error only contributes to the mass measurements.

For the cross-feed background to the $D_{sJ}(2317)$ signal, we vary the feed-down background parameters and the $D_{sJ}(2457)$ yield by $\pm 1\sigma$ and assign the variation in output values as errors. For the $D_{sJ}(2457)$, we determine the uncertainty of the feed-up fraction from the difference between the D_s^* signal region and the sideband region using the MC. For the non-cross-feed background, we repeat the fit using a second-order polynomial for the $D_{sJ}(2317)$ and a linear function for the $D_{sJ}(2457)$ and assign the difference as errors. Differences between the MC input and output values for the D_{sJ} parameters can reflect possible errors arising from the choice of signal shape and other factors in the analysis. We assign these differences as errors.

The final results for the masses are

$$\begin{aligned} M(D_{sJ}(2317)) &= 2317.2 \pm 0.5(\text{stat}) \pm 0.9(\text{syst}) \text{ MeV}/c^2 \\ M(D_{sJ}(2457)) &= 2456.5 \pm 1.3(\text{stat}) \pm 1.3(\text{syst}) \text{ MeV}/c^2. \end{aligned}$$

The $M(D_{sJ}(2317))$ result is consistent with BaBar [1] and CLEO results [2]. Our $M(D_{sJ}(2457))$ value is consistent with BaBar [17] but significantly lower than that from CLEO [2]. We set upper limits for the natural widths of $\Gamma(D_{sJ}(2317)) \leq 4.6 \text{ MeV}/c^2$ and $\Gamma(D_{sJ}(2457)) \leq 5.5 \text{ MeV}/c^2$ (90% C.L.), respectively.

Using the observed signal yields of $761 \pm 44(\text{stat}) \pm 30(\text{syst})$ and $126 \pm 25(\text{stat}) \pm 12(\text{syst})$ for the $D_{sJ}(2317)$ and $D_{sJ}(2457)$, and the detection efficiencies of 8.2% and 4.7% for the $D_{sJ}(2317)$ and $D_{sJ}(2457)$, we determine the ratio

$$\begin{aligned} &\frac{\sigma(D_{sJ}(2457)) \cdot \mathcal{B}(D_{sJ}^+(2457) \rightarrow D_s^{*+}\pi^0)}{\sigma(D_{sJ}(2317)) \cdot \mathcal{B}(D_{sJ}^+(2317) \rightarrow D_s^+\pi^0)} \\ &= 0.29 \pm 0.06(\text{stat}) \pm 0.03(\text{syst}). \end{aligned}$$

The detection efficiencies are determined from the MC assuming the same fragmentation function for the two states. The dominant source of systematic error is the systematic uncertainty in the $D_{sJ}(2457)$ yield.

In the $D_{sJ}(2457)$ region of the $\Delta M(D_s^+\pi^0)$ distribution, we find 22 ± 22 events from a fit to a possible $D_{sJ}(2457)$ signal. From this, we obtain the upper limit

$$\frac{\mathcal{B}(D_{sJ}^+(2457) \rightarrow D_s^+\pi^0)}{\mathcal{B}(D_{sJ}^+(2457) \rightarrow D_s^{*+}\pi^0)} \leq 0.21 \text{ (90\% C.L.)}.$$

The decay to a pseudo-scalar pair is allowed for a state with a parity of $(-1)^J$. Thus, absence of such a decay disfavors $D_{sJ}(2457)$ having J^P of 0^+ or 1^- .

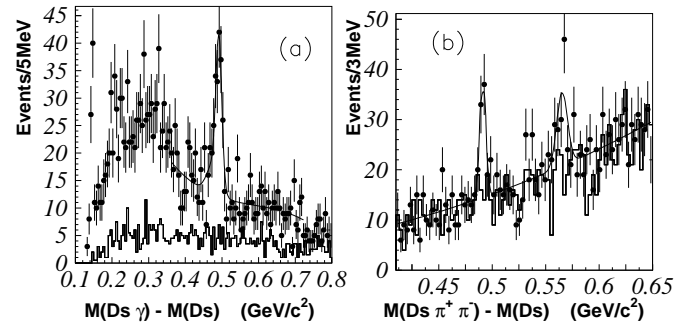


FIG. 3: (a) The $\Delta M(D_s^+\gamma)$ distribution. The curve is a fit using a double Gaussian for the signal and a third-order polynomial for the background. (b) The $\Delta M(D_s^+\pi^+\pi^-)$ distribution. The curve is a fit using Gaussian for the signals and a third-order polynomial for the background.

Figure 3(a) shows the $\Delta M(D_s^+\gamma) = M(D_s^+\gamma) - M_{D_s^+}$ distribution. Here photons are required to have energies greater than 600 MeV in the CM and those that form a π^0 when combined with another photon in the event are not used. A clear peak near $\Delta M(D_s^+\gamma) \sim 490 \text{ MeV}/c^2$, corresponding to the $D_{sJ}(2457)$, is observed. No peak is found in the $D_{sJ}(2317)$ region. The D_s^+ sideband distribution, shown as a histogram, shows no structure. We fit the distribution with a double Gaussian for the signal, which is determined from the MC, and a third-order polynomial for the background. The fit yields 152 ± 18 (stat) events and a ΔM peak at $491.0 \pm 1.3(\text{stat}) \pm 1.9(\text{syst}) \text{ MeV}/c^2$ (corresponding to $M = 2459.5 \pm 1.3(\text{stat}) \pm 2.0(\text{syst}) \text{ MeV}/c^2$). The $D_{sJ}(2457)$ mass determined here is consistent with the value determined from $D_s^*\pi^0$ decays.

Using the detection efficiency of 10.2% for the $D_s^+\gamma$ decay mode, we determine the branching fraction ratio

$$\frac{\mathcal{B}(D_{sJ}^+(2457) \rightarrow D_s^+\gamma)}{\mathcal{B}(D_{sJ}^+(2457) \rightarrow D_s^{*+}\pi^0)} = 0.55 \pm 0.13(\text{stat}) \pm 0.08(\text{syst}).$$

This result, which has a statistical significance of 10 σ , is consistent with the first measurement by Belle [16] $0.38 \pm 0.11(\text{stat}) \pm 0.04(\text{syst})$ with $B \rightarrow \bar{D}D_{sJ}(2457)$ decays, and with the theoretical predictions [3],[13]. The existence of the $D_{sJ}(2457) \rightarrow D_s\gamma$ mode rules out the 0^\pm quantum number assignments for the $D_{sJ}(2457)$ state. For the $D_{sJ}(2317)$, we obtain the upper limit

$$\frac{\mathcal{B}(D_{sJ}^+(2317) \rightarrow D_s^+\gamma)}{\mathcal{B}(D_{sJ}^+(2317) \rightarrow D_s\pi^0)} \leq 0.05 \text{ (90\% C.L.)}.$$

From the $M(D_s^{*+}\gamma) = M(D_s^{*+}\gamma) - M_{D_s^{*+}}$ distribution, we determine the upper limits

$$\frac{\mathcal{B}(D_{sJ}^+(2317) \rightarrow D_s^{*+}\gamma)}{\mathcal{B}(D_{sJ}^+(2317) \rightarrow D_s\pi^0)} \leq 0.18 \text{ (90\% C.L.)} \text{ and}$$

$$\frac{\mathcal{B}(D_{sJ}^+(2457) \rightarrow D_s^{*+}\gamma)}{\mathcal{B}(D_{sJ}^+(2457) \rightarrow D_s^{*+}\pi^0)} \leq 0.31 \text{ (90\% C.L.)}.$$

Figure 3(b) shows the $\Delta M(D_s^+\pi^+\pi^-) = M(D_s^+\pi^+\pi^-) - M_{D_s^+}$ distribution. For pions, we require at least one of them to have momentum greater than 300 MeV/c in the CM, one with $P(K/\pi) < 0.1$ and other with $P(K/\pi) < 0.9$, and $|M(\pi^+\pi^-) - M_{K_S}| \geq 15$ MeV/c². A clear peak near $\Delta M(D_s^+\pi^+\pi^-) \sim 490$ MeV/c², corresponding to the $D_{sJ}(2457)$, is observed. Evidence of an additional peak near $\Delta M(D_s^+\pi^+\pi^-) \sim 570$ MeV/c² corresponding to $D_{s1}(2536)$ is also visible. No peak is found in the $D_{sJ}(2317)$ region. The D_s^+ sideband distribution, shown as a histogram, shows no structure. We fit the distribution with Gaussians for the signals, which are determined from the MC, and a third-order polynomial for the background. The fit yields 59.7 ± 11.5 (stat) events and a ΔM peak at 491.4 ± 0.9 (stat) ± 1.5 (syst) MeV/c² (corresponding to $M = 2459.9 \pm 0.9$ (stat) ± 1.6 (syst) MeV/c²) for $D_{sJ}(2457)$, and 56.5 ± 13.4 (stat) events for $D_{s1}(2536)$. The statistical significance is 5.7σ for $D_{sJ}(2457)$, and 4.5σ for $D_{s1}(2536)$. This is the first observation of the $D_{sJ}(2457) \rightarrow D_s^+\pi^+\pi^-$ decay mode.

The existence of the $D_{sJ}(2457) \rightarrow D_s\pi^+\pi^-$ mode also rules out the 0^+ assignment for $D_{sJ}(2457)$. Using the detection efficiency of 15.8% for the $D_s\pi^+\pi^-$ decay mode, we determine the branching fraction ratio

$$\frac{\mathcal{B}(D_{sJ}^+(2457) \rightarrow D_s^+\pi^+\pi^-)}{\mathcal{B}(D_{sJ}^+(2457) \rightarrow D_s^{*+}\pi^0)} = 0.14 \pm 0.04(\text{stat}) \pm 0.02(\text{syst}),$$

where the systematic error is dominated by the systematic uncertainty of the $D_{sJ}(2457) \rightarrow D_s^{*+}\pi^0$ yield. We establish the upper limit

$$\frac{\mathcal{B}(D_{sJ}^+(2317) \rightarrow D_s^+\pi^+\pi^-)}{\mathcal{B}(D_{sJ}^+(2317) \rightarrow D_s^+\pi^0)} \leq 4 \times 10^{-3} \quad (90\% \text{ C.L.}).$$

Using the detection efficiency of 14.3% for the $D_{s1}(2536) \rightarrow D_s\pi^+\pi^-$ decay mode which assumes the same fragmentation function for the $D_{s1}(2536)$ and $D_{sJ}(2457)$, we establish the cross section times branching fraction ratio

$$\begin{aligned} & \frac{\sigma(D_{s1}(2536)) \cdot \mathcal{B}(D_{s1}^+(2536) \rightarrow D_s^+\pi^+\pi^-)}{\sigma(D_{sJ}(2457)) \cdot \mathcal{B}(D_{sJ}^+(2457) \rightarrow D_s^+\pi^+\pi^-)} \\ &= 1.05 \pm 0.32(\text{stat}) \pm 0.06(\text{syst}). \end{aligned}$$

In summary, we observe radiative and dipion decays of the $D_{sJ}(2457)$ and set upper limits on the corresponding decays of the $D_{sJ}(2317)$. We determine the $D_{sJ}(2317)$ and $D_{sJ}(2457)$ masses from their decays to $D_s^+\pi^0$ and $D_s^{*+}\pi^0$, respectively, and set an upper limit on the decay of $D_{sJ}(2457)$ to $D_s^+\pi^0$. These results are consistent

with the spin-parity assignments for the $D_{sJ}(2317)$ and $D_{sJ}(2457)$ of 0^+ and 1^+ , respectively.

We wish to thank the KEKB accelerator group for the excellent operation of the KEKB accelerator. We acknowledge support from the Ministry of Education, Culture, Sports, Science, and Technology of Japan and the Japan Society for the Promotion of Science; the Australian Research Council and the Australian Department of Education, Science and Training; the National Science Foundation of China under contract No. 10175071; the Department of Science and Technology of India; the BK21 program of the Ministry of Education of Korea and the CHEP SRC program of the Korea Science and Engineering Foundation; the Polish State Committee for Scientific Research under contract No. 2P03B 01324; the Ministry of Science and Technology of the Russian Federation; the Ministry of Education, Science and Sport of the Republic of Slovenia; the National Science Council and the Ministry of Education of Taiwan; and the U.S. Department of Energy.

* on leave from Nova Gorica Polytechnic, Nova Gorica

- [1] B. Aubert *et al.* (BaBar Collaboration), Phys. Rev. Lett. **90**, 242001 (2003).
- [2] D. Besson *et al.* (CLEO Collaboration), hep-ex/0305017.
- [3] W. Bardeen, E. Eichten, and C. Hill, hep-ph/0305049.
- [4] In the heavy c -quark approximation, one expects two doublets of $c\bar{s}$ states with quantum numbers $J^P = 0^+$, 1^+ ($j = 1/2$) and $J^P = 1^+$, 2^+ ($j = 3/2$). The second doublet has already been observed in DK and D^*K decays [5].
- [5] K. Hagiwara *et al.* (Particle Data Group), Phys. Rev. D **66**, 010001 (2002).
- [6] J. Bartelt and S. Shukla, Ann. Rev. Nucl. Part. Sci. **45** 133, (1995).
- [7] K. Abe *et al.* (Belle Collaboration), hep-ex/0307012.
- [8] R. Cahn and D. Jackson, hep-ph/0305012.
- [9] T. Barnes, F. Close and H. Lipkin, hep-ph/0305025.
- [10] E. Beveren and G. Rupp, hep-ph/0305035.
- [11] H. Cheng and W. Hou, hep-ph/0305038.
- [12] P. Colangelo and F. Fazio, hep-ph/0305040.
- [13] S. Godfrey, hep-ph/0305122.
- [14] A. Abashian *et al.* (Belle Collaboration), Nucl. Instr. and Meth. A **479**, 117 (2002).
- [15] S. Kurokawa and E. Kikutani *et al.*, Nucl. Instr. and Meth. A **499**, 1 (2003).
- [16] P. Krokovny *et al.* (Belle Collaboration), hep-ex/0308019, submitted to PRL.
- [17] A. Palano, hep-ex/0309028.